Information-theoretical approach to the many-particle hierarchy problem

Boris Melcher,[1] Boris Gulyak,[1,2] and Jan Wiersig[1]

[1]*Institut für Physik, Otto-von-Guericke-Universität Magdeburg, Postfach 4120, D-39016 Magdeburg, Germany*
[2]*Institut für Analysis und Numerik, Otto-von-Guericke-Universität Magdeburg, Postfach 4120, D-39016 Magdeburg, Germany*

We use the maximum entropy principle to circumvent the many-particle hierarchy problem that arises in conventional equation of motion techniques. Our efficient approach enables us to numerically determine the full density matrix of driven-dissipative quantum many-particle systems and gain access to all relevant expectation values and the full statistics and not only moments and correlation functions. We compare the maximum entropy method results with the numerically exact solution of the von Neumann-Lindblad equation for a four-level system resonantly coupled to one cavity mode and demonstrate excellent agreement in terms of entropy, mean photon number, autocorrelation function, and photon statistics. Moreover, we show that our approach can be used as a tool for learning about the relevant processes of quantum systems.

I. INTRODUCTION

Open quantum systems gained considerable attention due to their ability to make the very heart of the quantum world explorable. There, the interplay between driving mechanisms and dissipation processes strongly influences coherence properties of the probed system, leading to the investigation of, for instance, Bose-Einstein condensation of few photons [1], Schrödinger cats in photon resonators [2], superradiance of quantum dots (QDs) [3], cavity optomechanics [4], and the spin-boson model in superconducting quantum circuits [5].

Among many others [6] one common approach to describe those driven-dissipative quantum many-particle systems is to combine equations of motion (EoM) techniques with approximation schemes such as the cluster expansion method [7]. In doing so, a set of differential equations is derived describing the time evolution of several relevant quantum mechanical expectation values. Although this approach has been successfully applied to the microscopical description of exciton dynamics in quantum wells [8], photoluminescence [9–12], ultracold Bose gases [13], spin dynamics [14], cavity phonons [15], QD lasers [3,16–21], and many more, there are several down-sides to those techniques. Due to many-particle coupling an infinite hierarchy of differential equations unfolds that has to be truncated at a certain point. If not done carefully this can lead to unphysical behavior such as the occurrence of negative values for the photon autocorrelation function [7]. Consequently, the choice of truncation usually strongly depends on the investigated system. Moreover, EoM techniques only provide moments and correlation functions, but never the full statistics of quantum mechanical observables. Furthermore, the same moments and correlation function values are compatible to radically different statistics, so access to the full statistics is necessary to guarantee a clear physical understanding [18,22]. Although it is in principle possible to construct the full statistics out of moments alone [23] the full density matrix is still not at hand and the problem of truncating the infinite hierarchy remains.

In this paper, we use the maximum entropy method (MEM) to calculate the full density matrix and thus make all relevant expectation values and correlation functions as well as the full statistics directly accessible. Importantly, a truncation of the many-particle hierarchy in terms of factorization schemes is completely avoided. Instead, we use the knowledge about the stationarity of expectation values of several distinct observables and deduce the least biased density matrix. To test our approach, we compare the results for a four-level single QD microcavity laser where the full density matrix is still available by numerically solving the von Neumann-Lindblad (vNL) equation for the system of interest coupled to a Markovian environment. Although we restrict ourselves to one specific system the approach is neither limited to quantum optics nor to systems described by the vNL equation but can in principle be applied to all systems with stationary dynamics, i.e., in a steady state, but not necessarily in thermodynamic equilibrium.

II. MAXIMUM ENTROPY METHOD

The maximum entropy principle [24,25], originally introduced to derive the density matrix in equilibrium statistical mechanics, is nowadays used in various fields such as biophysics and nanoscience [26] and can straightforwardly be applied to the quantum case [27,28]. It basically answers the question: having given m pieces of incomplete information about a quantum system, what would be a reasonable guess for the density matrix ρ? The maximum entropy principle suggests to chose the one that has maximum entropy, and thus maximum indeterminateness or rather least bias, yet still accounts for all given constraints. The information usually comes as expectation values

$$\langle A_i \rangle = \mathrm{Tr}(\rho A_i), \quad i = 1, \ldots, m \tag{1}$$

for quantum mechanical operators A_i and might stem from experimental measurements or some other theory while the measure of indeterminateness is given by the von
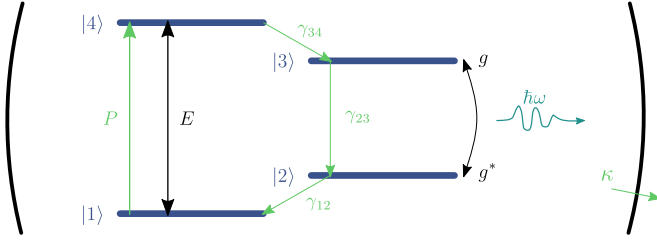
FIG. 1. Four-level QD in a microcavity. The electronic energy levels are denoted by $|1\rangle$, $|2\rangle$, $|3\rangle$, and $|4\rangle$. The inner levels are resonantly coupled to the cavity mode with frequency ω and light-matter coupling strength g. Interaction with the environment, namely electronic relaxation with rates γ_{ij}, cavity losses with rate κ and incoherent pumping with rate P are shown in lighter color. E represents an external field in the coherent pumping case.

Neumann entropy

$$S(\rho) = -\operatorname{Tr}(\rho \ln \rho). \qquad (2)$$

Alternatively, the procedure of entropy maximization can be seen as basic self-consistency requirement when drawing inferences form stochastic data [26,28]. Requiring the maximum entropy density matrix $\hat{\rho}$ (we use a hat to label the MEM density matrix) to fulfill the conditions

$$S(\hat{\rho}) = \max, \quad \operatorname{Tr}(\hat{\rho}) = 1, \quad \operatorname{Tr}(\hat{\rho}A_i) = \mu_i, \quad i = 1, \dots, k, \qquad (3)$$

where all input information is contained within the given expectation values μ_i leads to the maximum entropy density matrix

$$\hat{\rho} = \frac{1}{Z(\lambda)} \exp\left(-\sum_{i=1}^{m} \lambda_i A_i\right),$$

$$Z(\lambda) = \operatorname{Tr}\left[\exp\left(-\sum_{i=1}^{m} \lambda_i A_i\right)\right], \qquad (4)$$

where $Z(\lambda)$ is referred to as generalized partition function. The input information enters the maximum entropy density matrix via the Lagrange multipliers $\lambda_i = \lambda_i(\mu_1, \dots, \mu_m)$ that are functions of the given constraints. The main task is to find suitable Lagrange multipliers such that

$$\operatorname{Tr}[\hat{\rho}(\lambda)A_i] - \mu_i = 0, \quad i = 1, \dots, m, \qquad (5)$$

is fulfilled, which can be done using a standard nonlinear least-squares solver.

III. BENCHMARK MODEL

As a benchmark system we choose a four-level single QD microcavity laser (see Fig. 1 and Refs. [29–31]) where a single charge carrier from the ground state $|1\rangle$ is either pumped incoherently with a pump rate P or coherently excited via an external field E into the highest level $|4\rangle$. E is a pumping rate (in units of ps^{-1}) proportional to the field strength of the driving field. It then relaxes nonradiatively via the inner levels $|3\rangle$ and $|2\rangle$ with decay rates γ_{34}, γ_{23}, and γ_{12}, into the lowest level. The inner levels are resonantly coupled to the cavity mode with frequency ω and light-matter coupling strength g.

Cavity losses occur at a rate κ. In the interaction picture the interacting parts of the Hamiltonian read

$$H_{\text{JC}} = g^* a_2^\dagger a_3 b^\dagger + g a_3^\dagger a_2 b, \qquad (6)$$

$$H_E = i\hbar E(a_1^\dagger a_4 - a_4^\dagger a_1), \qquad (7)$$

where the Jaynes-Cummings Hamiltionian H_{JC} governs the light-matter interaction in electric dipole and rotating-wave approximation, while H_E represents the coherent pumping process via an external field, which is assumed to be in resonance with the transition of the outer electronic levels. In the equations above $a_i^\dagger$ and a_i are fermionic creation and annihilation operators that create or annihilate an electron in state $|i\rangle$ and $b^\dagger$ and b are bosonic photon creation and annihilation operators, respectively.

We focus on Markovian environments here by including coupling to external reservoirs via Lindblad terms with rates ϑ_i and associated Lindblad operators $c_i^\dagger$ and c_i resulting in the vNL master equation for the full density matrix ρ

$$\frac{d}{dt}\rho = -\frac{i}{\hbar}[H, \rho] + \sum_k \frac{\vartheta_k}{2}(2c_k\rho c_k^\dagger - c_k^\dagger c_k\rho - \rho c_k^\dagger c_k) \quad (8)$$

with $H = H_{\text{JC}} + H_E$. The summation runs over all included processes, namely electronic relaxation ($c_k \to a_i^\dagger a_j$, $\vartheta_k \to \gamma_{ij}$), cavity losses ($c_k \to b$, $\vartheta_k \to \kappa$) as well as incoherent pumping ($c_k \to a_4^\dagger a_1$, $\vartheta_k \to P$). For nonvanishing rates the system reaches a unique steady state [32]. We refer to Refs. [29,30,33] for a detailed discussion of the differences between incoherent and coherent pumping. Because of the small system size, here the vNL equation is still solvable numerically yielding the full density matrix ρ, which is in general not the case for larger systems.

IV. INPUT INFORMATION

Let us now review the concept of observation levels (OLs) and give remarks on the used input information. For successfully constructing a maximum entropy density matrix we require the expectation values $\mu_i = \langle A_i \rangle$ of a set of m quantum operators $\{\alpha\} = \{A_i : i = 1, \dots, m\}$. Following Ref. [27] we refer to $\hat{\rho}_{\{\alpha\}}$ constructed according to Eq. (4) as density matrix with respect to OL $\{\alpha\}$. Whether an OL is sufficient depends on the ability to predict the expectation values of other observables $\langle F \rangle = \operatorname{Tr}(\rho F) \approx \operatorname{Tr}(\hat{\rho}_{\{\alpha\}} F)$ with sufficient accuracy. Then the OL and therefore the choice of input information is physically reasonable.

In contrast to prior works [23,34] we do not use expectation values computed from EoM techniques here. Rather, we exploit that, in steady state, the expectation value of any observable B_i is constant in time. Hence, we use

$$\frac{d}{dt}\langle B_i \rangle = \left\langle \frac{dB_i}{dt} \right\rangle = 0, \quad i = 1, \dots, m \qquad (9)$$

as constraint [35], where the time evolution follows directly from Eqs. (1) and (8)

$$\frac{d}{dt}\langle B_i \rangle = \frac{i}{\hbar}\langle [H, B_i]\rangle + \sum_k \frac{\vartheta_k}{2}\langle 2c_k^\dagger B_i c_k - c_k^\dagger c_k B_i - B_i c_k^\dagger c_k\rangle. \qquad (10)$$

TABLE I. Added input information for the first four OLs {1}, {2}, {3}, and {4}. For each shown operator B_i we use $d\langle B_i \rangle/dt = 0$ with Eq. (10) as constraint. For higher OLs we also include the constraints of all previous orders. Operators in the rightmost column are only included for coherent pumping.

{1}	n	N_i	$i(a_2^\dagger a_3 b^\dagger - a_3^\dagger a_2 b)$	$a_1^\dagger a_4 + a_4^\dagger a_1$
{2}	n^2	nN_i	$i(na_2^\dagger a_3 b^\dagger - a_3^\dagger a_2 bn)$	$n(a_1^\dagger a_4 + a_4^\dagger a_1)$
{3}	n^3	$n^2 N_i$	$i(n^2 a_2^\dagger a_3 b^\dagger - a_3^\dagger a_2 bn^2)$	$n^2(a_1^\dagger a_4 + a_4^\dagger a_1)$
{4}	n^4	$n^3 N_i$	$i(n^3 a_2^\dagger a_3 b^\dagger - a_3^\dagger a_2 bn^3)$	$n^3(a_1^\dagger a_4 + a_4^\dagger a_1)$

With this choice of input information our approach does not depend on explicit numerical values for $\langle b^\dagger b \rangle$, etc., but can be applied as a stand-alone method where the EoM (10) themselves are used as constraints to derive the full density matrix in the steady state. Note that we neither need to solve the EoM nor to close the set of EoM by truncating the many-particle hierarchy.

The choice of included operators follows naturally from the observables of interest and the right-hand side of Eq. (10). Here we consider the linearly independent operators n, N_1, N_2, N_3, and N_4 where $n = b^\dagger b$ and $N_i = a_i^\dagger a_i$ are the occupation number operators as well as the photon-assisted polarization $i(a_2^\dagger a_3 b^\dagger - a_3^\dagger a_2 b)$. Congruously, we also take into account $a_1^\dagger a_4 + a_4^\dagger a_1$ for coherently pumped systems. For higher OLs we successively multiply the operators from the previous order with n. This leads to a set of 6(7) pieces of information and an equal number of Lagrange multipliers for the first OL, 12(14) for the second, 18(21) for the third, and 24(28) for the fourth (see Table I). For $\hat{\rho}$ to have the characteristics of a density matrix all given combinations of operators are required to be self-adjoint and thus represent physical observables. This also ensures the Lagrange multipliers to be real. Any linear combination of the above-mentioned input information leads to the same maximum entropy density matrix [27].

V. NUMERICAL RESULTS

To benchmark the MEM results we compare $\hat{\rho}$ to the full steady-state density matrix obtained by numerically solving the vNL equation (8) for a range of coherent and incoherent pump rates. It should be emphasized that both chosen methods are radically different and do not rely on each other. Note that also other approaches, such as a variational principle [36] or computing the kernel of the Liouvillian [37], can be applied to determine the steady state. For numerical implementation we restrict the photonic Hilbert space to $n_{\max} = 40$ and only store the nonzero elements of the sparse square 164×164 density matrix. We stress that no time evolution has to be calculated using the MEM.

Providing more information, i.e., increasing the OL, in general leads to a density matrix with less entropy thus less uncertainty $S(\hat{\rho})$ (cf. Fig. 2). The entropy decreases for higher OLs and finally tends towards the numerically exact steady-state solution of the vNL equation. This is true for all pump rates for both coherently and incoherently pumped systems. For higher pump rates a higher OL is required, whereas for low pump rates even the first OL is sufficient. To measure the
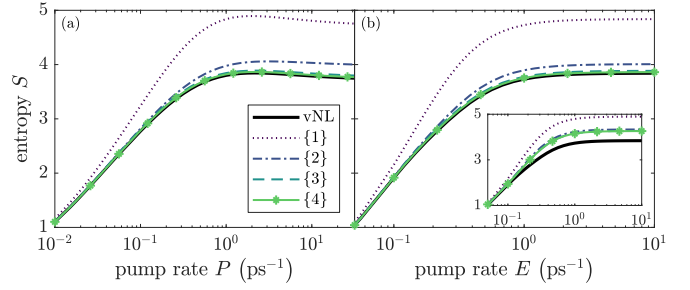

FIG. 2. Entropy S for (a) incoherent and (b) coherent pumping. Solid black curves show $S(\rho)$ for the steady-state solution of the vNL equation. Other curves show $S(\hat{\rho}_{\{\alpha\}})$ for the first four OLs. For the inset in (b) input information of the type $a_1^\dagger a_4 + a_4^\dagger a_1$ was excluded. Throughout all calculations we use the following parameters: $\gamma_{12} = \gamma_{34} = 1\,\mathrm{ps}^{-1}$, $\gamma_{23} = 0.01\,\mathrm{ps}^{-1}$, $\kappa = 0.02\,\mathrm{ps}^{-1}$, and $g = 0.2\,\mathrm{meV}$.

quality of the maximum entropy density matrix $\hat{\rho}$ compared to the numerically exact ρ we use the quantum relative entropy

$$S(\rho||\hat{\rho}) = \mathrm{Tr}[\rho(\ln\rho - \ln\hat{\rho})]. \qquad (11)$$

It measures how much information is lost when choosing the approximation $\hat{\rho}$ instead of the exact density matrix ρ. Alternatively, one could use the trace distance $T(\rho, \hat{\rho})$. Both are connected via the quantum Pinsker inequality $S(\rho||\hat{\rho}) \geqslant 2[T(\rho, \hat{\rho})]^2$ [38]. Higher OLs lead to a decrease of relative entropy hence the maximum entropy density matrix $\hat{\rho}$ tends towards the density matrix ρ of the steady-state solution of the vNL equation (see Fig. 3).

The insets in Figs. 2 and 3 show that an appropriate choice of input information indeed is essential. There, the results are depicted when information about the stationarity of the coherent pumping process and its correlations is missing, hence input information of the form $a_1^\dagger a_4 + a_4^\dagger a_1$ is not included throughout all OLs (cf. Table I). Withholding it dramatically effects the results for the coherently pumped system, yielding less approximation quality, whereas for incoherent pumping this information is completely obsolete. Even explicitly adding it leads to vanishing of the corresponding Lagrange multipliers throughout the whole range of pump rates and for all OLs. This corresponds to the notion that in the incoherent excitation regime averages of the form $\langle a_1^\dagger a_4 \rangle$ and $\langle a_4^\dagger a_1 \rangle$ vanish [17,39]. In that sense the MEM can be understood as a trial-and-error method for learning and identifying the relevant processes within physical systems.
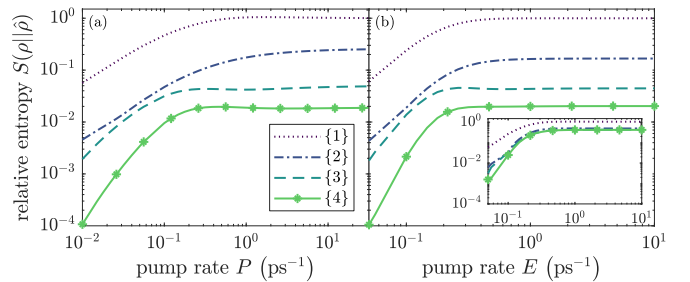

FIG. 3. Relative entropy $S(\rho||\hat{\rho}_{\{\alpha\}})$ for (a) incoherent and (b) coherent pumping up to fourth OL. For the inset in (b) input information of the type $a_1^\dagger a_4 + a_4^\dagger a_1$ was excluded.
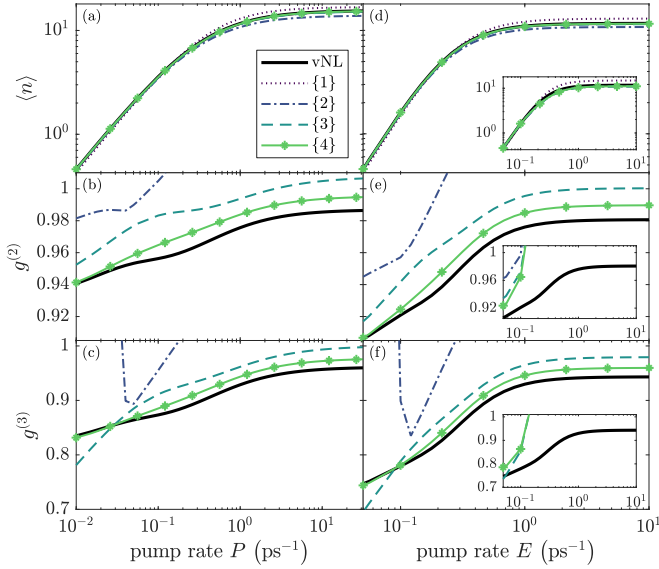
FIG. 4. Mean photon number $\langle n \rangle$ [(a) and (d)] and second- and third-order autocorrelation function $g^{(2)}$ [(b) and (e)] and $g^{(3)}$ [(c) and (f)] for (a)–(c) incoherent and (d)–(f) coherent pumping. Solid black curves show the results for the steady-state solution of the vNL equation. Other curves show the MEM results for the first four OLs. For the insets in (d)–(f) input information of the type $a_1^\dagger a_4 + a_4^\dagger a_1$ was excluded.

From the full density matrix, relevant physical observables, namely the mean photon number $\langle n \rangle = \langle b^\dagger b \rangle$ and autocorrelation functions $g^{(k)}(0) = \langle (b^\dagger)^k b^k \rangle / \langle b^\dagger b \rangle^k$ are directly accessible, see Fig. 4. Contrary to naive expectation, for low pump rates the second-order autocorrelation function is not close to zero because of the high-quality mode and the associated low loss rate. For a higher loss rate though, $g^{(2)}(0)$ is close to zero and the QD microcavity system operates as single-photon source.

Although the mean photon number already accords well within the first OL (cf. Fig. 4), to obtain reasonable values for the autocorrelation functions one needs to include higher-order moments. While OL $\{\alpha\}$ contains information about the stationarity of operators of the form $n^{(\alpha-1)}\tilde{B}_i$ (cf. Table I), the autocorrelation function of order k contains information about moments $\langle n^k \rangle$. Hence, to get good accordance for $g^{(k)}$, OL $\{k+1\}$ is sufficient. For lower pump rates though, we observe the autocorrelation functions to behave quite oddly [cf. second OL in Figs. 4(c) and 4(f)]. This is due to the restriction of the maximum photon number n to a finite value $n_{\max}$ that leads to an artificial increase of the probability values p_n close to $n_{\max}$. This results in an overestimation of higher-order moments that is highly dependent on the choice of $n_{\max}$. A truncation closer to the relevant part of the photon distribution (e.g., $n_{\max} = 10$) leads to better accordance for low pump rates as well. A more detailed discussion on the problem of restricting the maximum entropy distribution to a finite range can be found in Ref. [23]. We point out that the Lagrange multipliers are system-size dependent throughout all OLs. Nevertheless, for intermediate and high pump rates the values for entropy, relative entropy, various expectation values as well as the photon statistics remain almost unchanged for different choices of $n_{\max}$.
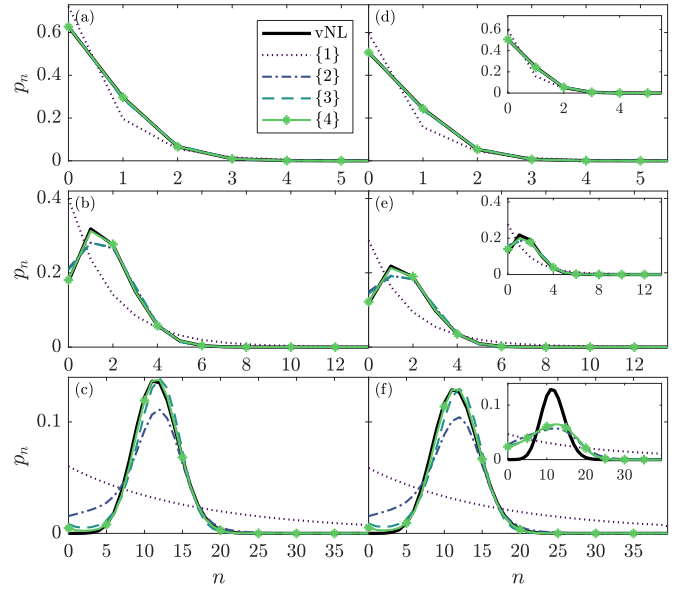

FIG. 5. Photon statistics p_n for pump rates (a) $P = 0.01\,\mathrm{ps}^{-1}$, (b) $P = 0.04\,\mathrm{ps}^{-1}$, (c) $P = 1\,\mathrm{ps}^{-1}$ for incoherent pumping, and (d) $E = 0.05\,\mathrm{ps}^{-1}$, (e) $E = 0.1\,\mathrm{ps}^{-1}$, (f) $E = 10\,\mathrm{ps}^{-1}$ for coherent pumping, respectively. Solid black curves show the photon statistics for the steady-state solution of the vNL equation. Other curves show p_n obtained by the MEM for the first four OLs. For the insets in (d)–(f) input information of the type $a_1^\dagger a_4 + a_4^\dagger a_1$ was excluded. In (a) and (d) the steady-state solution and the results for second, third, and fourth OL nearly lie on top of each other.

For both coherent and incoherent pumping, the MEM photon statistics tend towards the steady-state solution of the vNL equation (Fig. 5). Remarkably, already the second OL reproduces the photon statistics for low pump rates. For higher pump rates though, more information is required to reproduce the more complicated structure of the photon statistics; but still, the third OL distribution resembles the steady-state solution. Only for low photon numbers n the MEM tends to overestimate the probability p_n. In the case of insufficient information (see insets) only low pump rates are in agreement, whereas for higher pumping the MEM solution is far away from the original one. This fact again can be interpreted as a hint that operators of the form $a_1^\dagger a_4 + a_4^\dagger a_1$ are of crucial importance especially for stronger coherent pumping while being less important for weak pumping and completely obsolete in the incoherent pumping case.

VI. CONCLUSION

We demonstrated how the MEM can be used to derive the full density matrix of open quantum systems completely independent of EoM techniques and without the need for neither any factorization-based truncation schemes concerning the many-particle hierarchy nor a costly time integration. Instead, we used a finite set of input information leading to a self-consistent inference for the least biased full density matrix. As a benchmark we compared MEM results to the steady-state (but thermodynamical nonequilibrium) solution for a single QD microcavity laser described by a vNL equation for both coherent and incoherent pumping. By computing the entropy,

relevant expectation values, and the full photon statistics we demonstrated remarkable accordance and showed how the MEM can be used as trial-and-error method for learning about the relevant physical processes within the system. We point out the possibility to treat non-Markovian situations (see, e.g., Ref. [40]), where one would also include observables from the environment as input information. Furthermore, for systems with multiple steady states, the MEM would result in a unique unbiased mixture of the corresponding steady states, which is a considerable advantage whenever the initial state is not known. Consequently, the MEM opens up the possibility to circumvent numerous down-sides of EoM techniques, gives an information theoretical perspective on the infinite many-particle hierarchy and provides the full density matrix making the full statistics and all relevant operators directly accessible.

[1] B. T. Walker, L. C. Flatten, H. J. Hesten, F. Mintert, D. Hunger, A. A. P. Trichet, J. M. Smith, and R. A. Nyman, Nat. Phys. **14**, 1173 (2018).

[2] F. Minganti, N. Bartolo, J. Lolli, W. Casteels, and C. Ciuti, Sci. Rep. **6**, 26987 (2016).

[3] F. Jahnke, C. Gies, M. Aßmann, M. Bayer, H. A. M. Leymann, A. Foerster, J. Wiersig, C. Schneider, M. Kamp, and S. Höfling, Nature Commun. **7**, 11540 (2016).

[4] M. Aspelmeyer, T. J. Kippenberg, and F. Marquardt, Rev. Mod. Phys. **86**, 1391 (2014).

[5] L. Magazzù, P. Forn-Díaz, R. Belyansky, J.-L. Orgiazzi, M. A. Yurtalan, M. R. Otto, A. Lupascu, C. M. Wilson, and M. Grifoni, Nature Commun. **9**, 1403 (2018).

[6] I. de Vega and D. Alonso, Rev. Mod. Phys. **89**, 015001 (2017).

[7] H. A. M. Leymann, A. Foerster, and J. Wiersig, Phys. Rev. B **89**, 085308 (2014).

[8] W. Hoyer, M. Kira, and S. W. Koch, Phys. Rev. B **67**, 155113 (2003).

[9] M. Kira, F. Jahnke, and S. W. Koch, Phys. Rev. Lett. **81**, 3263 (1998).

[10] N. Baer, C. Gies, J. Wiersig, and F. Jahnke, Eur. Phys. J. B **50**, 411 (2006).

[11] T. Feldtmann, L. Schneebeli, M. Kira, and S. W. Koch, Phys. Rev. B **73**, 155319 (2006).

[12] M. Florian, C. Gies, F. Jahnke, H. A. M. Leymann, and J. Wiersig, Phys. Rev. B **87**, 165306 (2013).

[13] T. Köhler and K. Burnett, Phys. Rev. A **65**, 033601 (2002).

[14] M. D. Kapetanakis and I. E. Perakis, Phys. Rev. Lett. **101**, 097201 (2008).

[15] J. Kabuss, A. Carmele, T. Brandes, and A. Knorr, Phys. Rev. Lett. **109**, 054301 (2012).

[16] S. Ritter, P. Gartner, C. Gies, and F. Jahnke, Opt. Express **18**, 9909 (2010).

[17] C. Gies, J. Wiersig, M. Lorke, and F. Jahnke, Phys. Rev. A **75**, 013803 (2007).

[18] H. A. M. Leymann, C. Hopfmann, F. Albert, A. Foerster, M. Khanbekyan, C. Schneider, S. Höfling, A. Forchel, M. Kamp, J. Wiersig, and S. Reitzenstein, Phys. Rev. A **87**, 053819 (2013).

[19] M. Khanbekyan, H. A. M. Leymann, C. Hopfmann, A. Foerster, C. Schneider, S. Höfling, M. Kamp, J. Wiersig, and S. Reitzenstein, Phys. Rev. A **91**, 043840 (2015).

[20] M. Fanaei, A. Foerster, H. A. M. Leymann, and J. Wiersig, Phys. Rev. A **94**, 043814 (2016).

[21] H. A. M. Leymann, A. Foerster, F. Jahnke, J. Wiersig, and C. Gies, Phys. Rev. Appl. **4**, 044018 (2015).

[22] E. Schlottmann, M. von Helversen, H. A. M. Leymann, T. Lettau, F. Krüger, M. Schmidt, C. Schneider, M. Kamp, S. Höfling, J. Beyer, J. Wiersig, and S. Reitzenstein, Phys. Rev. Appl. **9**, 064030 (2018).

[23] B. Gulyak, B. Melcher, and J. Wiersig, Phys. Rev. A **98**, 053857 (2018).

[24] E. T. Jaynes, Phys. Rev. **106**, 620 (1957).

[25] E. T. Jaynes, Phys. Rev. **108**, 171 (1957).

[26] S. Pressé, K. Ghosh, J. Lee, and K. A. Dill, Rev. Mod. Phys. **85**, 1115 (2013).

[27] E. Fick and G. Sauermann, *The Quantum Statistics of Dynamic Processes* (Springer, 1990).

[28] J. Shore and R. Johnson, IEEE Trans. Inf. Theory **26**, 26 (1980).

[29] T. C. Ralph and C. M. Savage, Phys. Rev. A **44**, 7809 (1991).

[30] Y. Mu and C. M. Savage, Phys. Rev. A **46**, 5944 (1992).

[31] I. H. Grothe, Theoretisches Modell der Quantenspektroskopie an Einzelatomen, Bachelor's thesis, Universität Bremen, 2014.

[32] S. G. Schirmer and X. Wang, Phys. Rev. A **81**, 062306 (2010).

[33] C. Gies, M. Florian, A. Steinhoff, and F. Jahnke, *Quantum Dots for Quantum Information Technologies* (Springer International Publishing, Berlin, 2017), pp. 3–40.

[34] T. Lettau, H. A. M. Leymann, B. Melcher, and J. Wiersig, Phys. Rev. A **97**, 053835 (2018).

[35] B. Gulyak, Maximum-Entropie-Methoden in der Vielteilchenphysik, Diploma thesis, Otto-von-Guericke-Universität Magdeburg, 2016.

[36] H. Weimer, Phys. Rev. Lett. **114**, 040402 (2015).

[37] C. Navarrete-Benlloch, arXiv:1504.05266.

[38] F. Hiai, M. Ohya, and M. Tsukada, Pacific J. Math. **96**, 99 (1981).

[39] P. Gartner, Phys. Rev. B **99**, 115313 (2019).

[40] L. A. Pachón and P. Brumer, Phys. Rev. A **87**, 022106 (2013).